RSC Advances

PAPER

View Article Online
View Journal | View Issue

Cite this: *RSC Adv.*, 2019, **9**, 6583

A novel route to the synthesis of an Fe_3O_4/h-BN 2D nanocomposite as a lubricant additive

Jun Zhao,[*a] Guangyan Chen,[b] Yongyong He,[b] Shuangxi Li,[a] Zhiqiang Duan,[*c] Yingru Li[d] and Jianbin Luo[b]

Received 16th December 2018
Accepted 31st January 2019

DOI: 10.1039/c8ra10312g

rsc.li/rsc-advances

Two-dimensional (2D) nanocomposites as lubricant additives have been widely studied, but the synthetic process of the nanocomposites is not always environmentally friendly or economical. In this study, a new 2D nanocomposite, Fe_3O_4/h-BN, has been prepared by physical mixing of exfoliated h-BN nanosheets and organically modified Fe_3O_4 nanoparticles. The nanocomposite displays a unique 2D-layered structure without folds or wrinkles. The Fe_3O_4 nanoparticles are uniformly dispersed on the h-BN nanosheet surfaces with the help of an elegant self-assembly strategy from van der Waals interactions. For the first time, Fe_3O_4/h-BN is studied as a lubricant additive and it exhibits excellent tribological properties. The coefficient of friction (COF) and the wear depth can be respectively reduced by 47% and 80% compared with the base oil. Based on the advantages of a simple and low-cost synthetic process and significant tribological properties, Fe_3O_4/h-BN offers great potential for lubrication application.

Introduction

Lubrication is the most efficient way to reduce friction energy consumption. As crucial components of lubricants, lubricant additives can increase the working life of machinery and promote remarkable energy savings by orders of magnitude. Nowadays, two-dimensional (2D) nanomaterials as lubricant additives have attracted more and more attention because of their unique atom-thick 2D structure, good physical and chemical stability, and excellent mechanical and thermal properties. 2D nanomaterial additives[1–4] such as h-BN, graphene, MoS_2, *etc.* effectively enter the contact areas during sliding, and prevent the direct contact of rubbing surfaces. Their adjacent layers bonded by weak van der Waals force, can slide easily against each other, which further reduces friction and wear.[3,5–7]

Recently, considerable efforts have been made to fabricate 2D nanocomposite lubricant additives, such as Cu/graphene, Fe_2O_3/graphene and Al_2O_3/nanotube, *etc.*[8–11] The 2D nanocomposites show better dispersion and lubrication properties than pure 2D nanomaterials, because the nanocomposites are able to disperse uniformly in lubricants and can form a synergetic protective tribofilm on the rubbing surfaces.[9,12–14] However, the synthetic process of the nanocomposites is not always environment friendly or economical, and some harmful or toxic oxidants and reductants such as concentrated sulfuric acid and hydrazine hydrate are unavoidable. By contrast, h-BN with good mechanical properties, thermal conductivity and stable oxidation resistance also attracts much attention,[15–17] and lately, h-BN nanocomposites have been achieved by simple and green routes in our recent studies.[18,19] However, h-BN nanocomposite as a lubricant additive haven't been studied. The tribological properties of h-BN nanocomposite in comparison with pure h-BN are still unknown.

In this study, we proposed a novel route to synthesis of Fe_3O_4/h-BN 2D nanocomposite lubricant additive. The nanocomposite was prepared by liquid-phase exfoliation and physical compositing process, characterized by high-resolution transmission electron microscopy (HRTEM), X-ray diffractometer (XRD) and X-ray photoelectron spectroscopy (XPS). The tribological properties of the nanocomposites were studied by using a reciprocating sliding tester. This study offers an efficient 2D nanocomposite additive for lubrication application, and also shows significant meaning because of simple and low-cost synthetic process.

Experimental

2D nanomaterials can be directly exfoliated by sonication in some organic solvents. *N*-Methyl-2-pyrrolidinone (NMP) is good solvent for exfoliation of h-BN, because the Hansen solubility parameters of NMP match that of h-BN well.[20] Therefore, the initial h-BN sheet was firstly dispersed in the NMP by magnetic

[a]*College of Mechanical and Electrical Engineering, Beijing University of Chemical Technology, Beijing 100029, China. E-mail: zhaojun@mail.buct.edu.cn*
[b]*State Key Laboratory of Tribology, Tsinghua University, Beijing, 100084, China*
[c]*Electronics and Information Engineering College, Hunan University of Science and Engineering, Yongzhou, Hunan 425199, China. E-mail: zqduan_1995@163.com*
[d]*Institute of Materials, China Academy of Engineering Physics, PO Box 9071-11, 621908, Mianyang, Sichuan, China*

stirring for 30 min, and then subjected to sonication for 30 h. The h-BN slurry was centrifuged at 4000 rpm for 10 min, of which the top half was vacuum-filtered and collected. After that, the exfoliated h-BN nanosheets was mixed in tetrahydrofuran (THF) at a concentration of 0.1 mg mL^{-1} with sonication for 1 h. The organically modified Fe_3O_4 nanoparticles prepared in our previous study,[19] were slowly added in the mixture, and then sonicated for 10 h, followed by vacuum-filtered, washed and vacuum-dried at 50 °C for 10 h, as shown in Fig. 1.

The structure characteristic of Fe_3O_4/h-BN was obtained by TEM (JEM-2010, Japan), XRD (Bruker, USA) and XPS (Thermo Fisher Scientific, USA). Friction tests were carried out by a reciprocating sliding tester (UMT-3 CETR, USA) with a load of 2 N (Hertz contact pressure is 1 GPa) shown in Fig. 1. The average sliding velocities are from 3 mm s^{-1} to 48 mm s^{-1}. The steel disc and steel ball (∅4 mm) were used as friction pairs, and the wear morphologies of the friction pairs were observed and analyzed by a white-light interferometer (MICROXAM-3D, America), SEM (FEI Quanta 200 FEG, Netherlands), AFM (Nanocute/E-SWEEP, Japan) and the XPS.

Results and discussion

As shown in Fig. 2(a), the h-BN in the Fe_3O_4/h-BN shows thin lamellar structure, and the Fe_3O_4 nanoparticles are richly loaded on the surface of the h-BN. The pure h-BN nanosheets display obvious layered structure as similar to the Fe_3O_4/h-BN (Fig. 2(b)). The pristine Fe_3O_4 nanoparticles (ChaoWei Nanotechnology Co., Ltd., Shanghai, China) display spherical structure and they are prone to agglomeration as shown in Fig. 2(c). According to the TEM images of the Fe_3O_4/h-BN (Fig. 2(d) and (e)), the exfoliated h-BN nanosheets displays unique 2D-layered structure without any folds or wrinkles. The Fe_3O_4 nanoparticles are uniformly dispersed on the h-BN nanosheet surfaces with the help of an elegant self-assembly strategy from van der Waals interactions, which is attributed to the spontaneous attraction between the h-BN surfaces and the nanoparticles through van der Waals forces.[19] The nanoparticles shows quasi-spherical structure, of which the size distribution varies from 2 nm to 7 nm and the average diameter is about 4 nm as shown in the inset of Fig. 2(d). The obtained lattice distance of 0.48 nm closely matches the (111) plane of Fe_3O_4, The crystallographic structure of Fe_3O_4/h-BN is also characterized by XRD as shown in Fig. 2(f), in which the pure h-BN nanosheets (XFNANO Co., Ltd., Nanjing, China) are used for comparison. It can be seen that the five diffraction peaks in Fig. 2(f) at 26.88°, 41.66°, 43.91°, 50.16°and 55.20° are attributed to the (002), (100), (101), (102) and (004) reflections of the nature planes of h-BN, which is in accordance with reference data of the JCPDS card no. 34-042. The five peaks of Fe_3O_4/h-BN at 30.20°, 35.56°, 53.69°, 57.20° and 62.84° are assigned to (200), (311), (422) and (440) reflections of Fe_3O_4 in accordance with reference data of the JCPDS card no. 19-0629.[21] In addition, the XPS spectra of the Fe 2p, B 1s and N 1s in Fe_3O_4/h-BN are shown in Fig. 2(g)–(i). It can be seen that the Fe 2p spectrum displays two peaks at 711.00 eV and 724.75 eV, which are assigned to Fe 2p3/2 and 2p1/2, respectively, while the satellite peak at around 719 eV isn't obtained, meaning there is little Fe_2O_3 in the Fe_3O_4/h-BN. The remarkable peaks at 190.10 eV and 396.80 eV in the Fe_3O_4/h-BN are essentially attributed to the B 1s and N 1s spectra of h-BN. The B 1s spectrum of the Fe_3O_4/h-BN shows a single peak, which means that the Fe_3O_4/h-BN is highly pure, because there are no any bonds of B–O or B–S at lower binding energies.[19]

The tribological properties of lubricants can be dramatically improved when the content of nano-additives was 0.5 wt% in our previous studies,[22–24] so 0.5 wt% content of the Fe_3O_4/h-BN was used to study its tribological properties in this study. The suspension of Fe_3O_4/h-BN additive in lubricant was thorough mixed by a magnetic stirrer for 2 hours and then ultrasonic mixing for 30 min at room temperature. As shown in Fig. 3, the pristine Fe_3O_4 nanoparticles shows severe agglomeration after

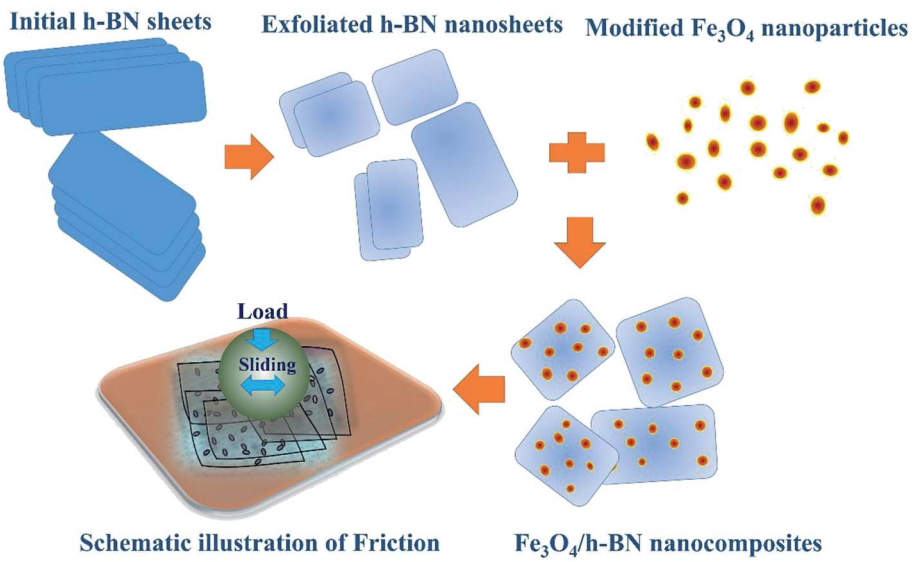

Fig. 1 Schematic illustration of synthesis route and friction test.

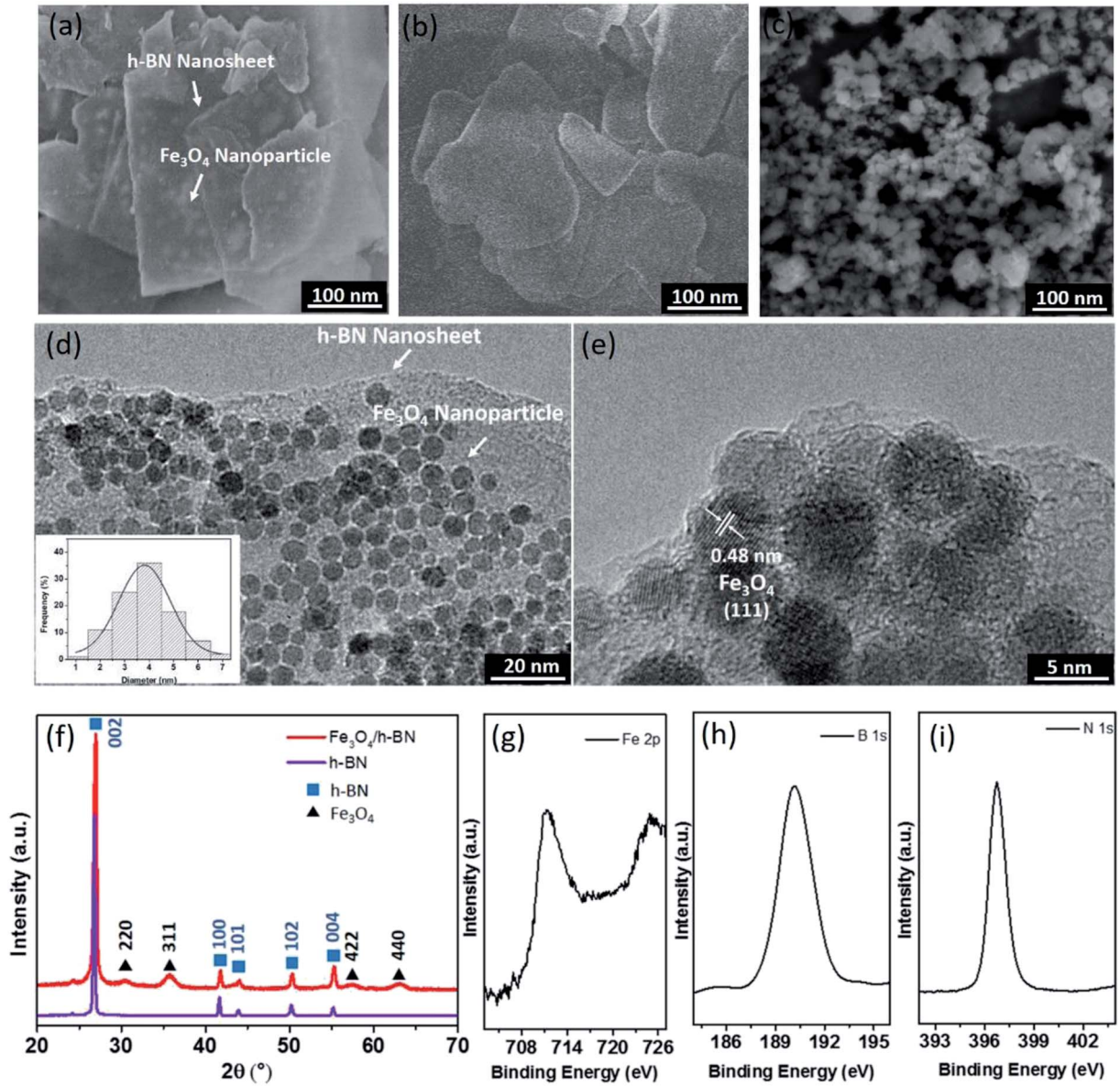

Fig. 2 SEM images of Fe_3O_4/h-BN nanocomposites (a), pure h-BN nanosheets (b) and pristine Fe_3O_4 nanoparticles (c); TEM images of Fe_3O_4/h-BN (d and e), inset in image (d) is the corresponding size distribution histogram. XRD pattern (f) of Fe_3O_4/h-BN and pure h-BN. XPS spectra of Fe_3O_4/h-BN, Fe 2p (g), B 1s (h) and N 1s (i).

20 h standing. The apparent sediment of pure h-BN was observed, while the Fe_3O_4/h-BN nanocomposites show stable dispersion state. The Fe_3O_4/h-BN has good self-dispersion stability in the base oil (PAO 6) because the Fe_3O_4 nanoparticles on the h-BN surfaces can decrease the van der Waals attraction between the Fe_3O_4/h-BN, which thereby can self-disperse in the lubricant.[8]

As shown in Fig. 4, the coefficient of friction (COF) of Fe_3O_4/h-BN is as low as 0.095 and is reduced by 47% compared with that of base oil. The COF of the base oil displays tempestuously fluctuant during running-in period, and its average value is as high as 0.18. When the h-BN nanosheets are added to the base oil, the COF is effectively reduced to about 0.13, but compared with Fe_3O_4/h-BN, the COF of h-BN is much higher and more unstable. The lubrication properties of these additives under different sliding velocities are then studied as displayed in Fig. 4(b). The COF of Fe_3O_4/h-BN keeps a highly stable level and their values are slightly below 0.1 under different sliding velocity. The COFs of the base oil and the h-BN decrease gradually with the increase of sliding velocity, and these values almost are close to that of the Fe_3O_4/h-BN at the sliding velocity of 48 mm s^{-1}, meaning that hydrodynamic lubrication effect works at higher sliding velocity.[24] However, the lubrication property of the h-BN is a little worse than the base oil at higher sliding velocity, probably because the adsorbing tribofilm of the h-BN on the friction interface is unstable and prone to being destroyed. For the pristine Fe_3O_4 nanoparticles, the COF is a little higher than that of base oil in spite of sliding velocities

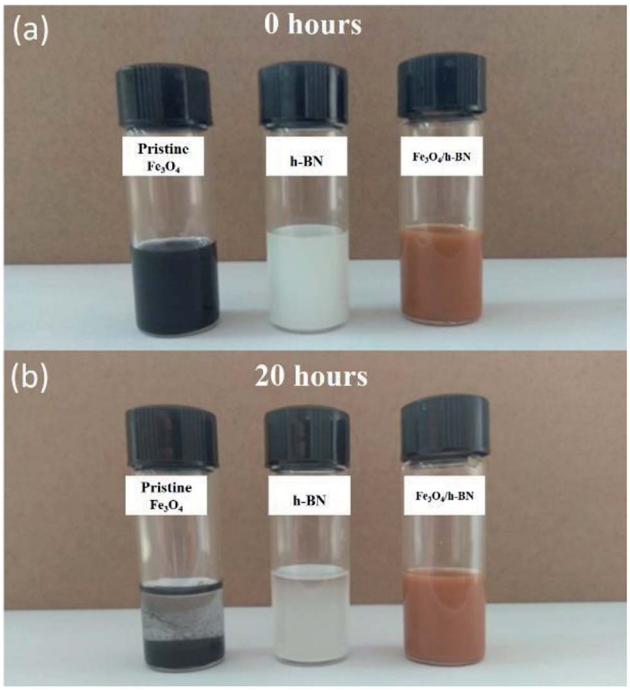

Fig. 3 Dispersion stability of pristine Fe_3O_4 nanoparticles, pure h-BN and Fe_3O_4/h-BN nanocomposites (0.5 wt%).

(Fig. 4(a) and (b)), which means the lubrication property of Fe_3O_4 is poor. It is probably because the nanoparticles display high surface activity and are prone to resulting in agglomeration and obstructing the sliding process. According to the cross sections of wear tracks shown in Fig. 4(c), the anti-wear property of the Fe_3O_4/h-BN is the best, because there are few materials removed from the rubbing surface. Although the h-BN displays better anti-wear property than the base oil, the rubbing surfaces lubricated by the h-BN suffer obvious scratches, of which the roughness is very high. Compared with the base oil, the wear depth of rubbing disc surfaces and the wear diameter of rubbing balls are respectively reduced by 80% and 60% with the lubrication of the Fe_3O_4/h-BN as shown in Fig. 4(d).

According to Fig. 5(a)–(l), the anti-wear property of the base oil is the worst because many severe abrasive scratches are formed on the rubbing balls and disc surfaces. There are a little slender tracks on the rubbing surfaces lubricated by the Fe_3O_4/h-BN, while that lubricated by the h-BN shows wide furrows. Furthermore, it can be seen that there are obvious scratches and severe adhesion occurred on the rubbing surfaces lubricated by the base oil based on the SEM and AFM results (Fig. 5(c) and (d)), which means the friction pairs mainly suffer abrasive and adhesive wear due to the direct contact of rubbing surfaces.[24] The rubbing surface lubricated by the h-BN displays much more severe abrasive wear, probably because the h-BN is prone to being agglomeration and can't effectively enter into contact

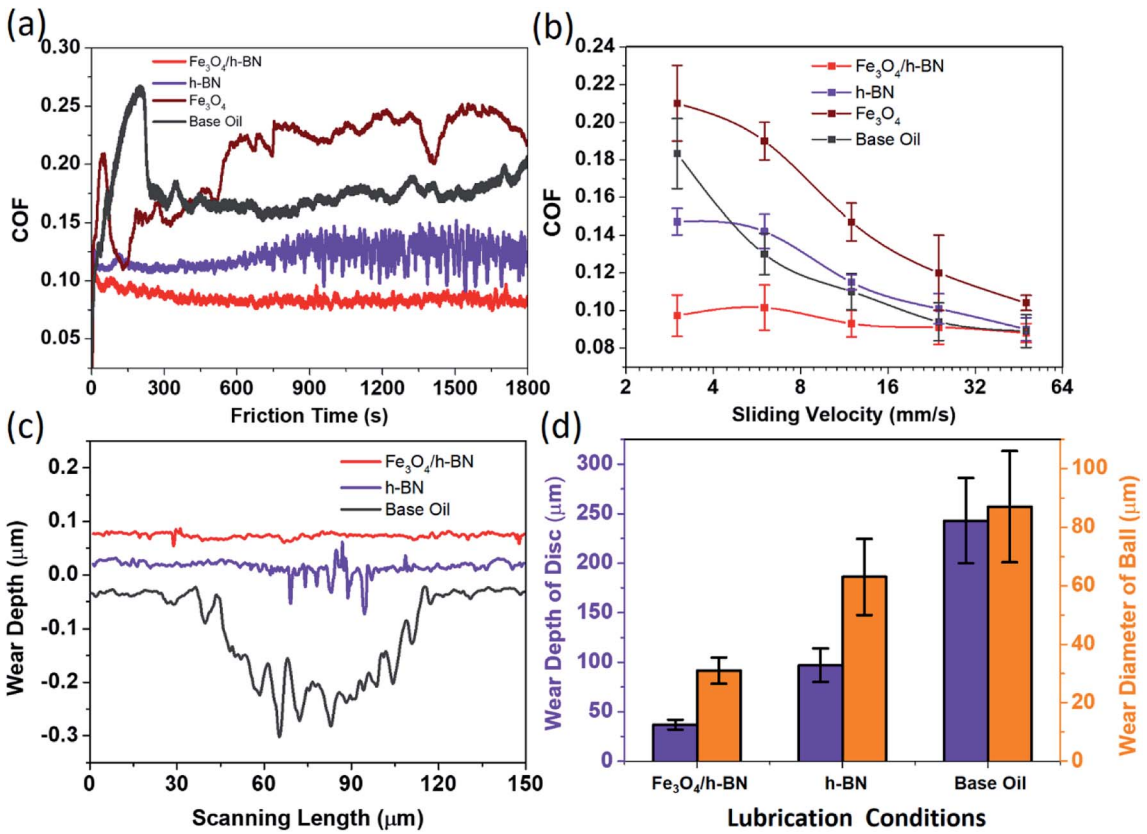

Fig. 4 COFs of Fe_3O_4/h-BN (0.5 wt%) and pure h-BN (0.5 wt%), pristine Fe_3O_4 (0.5 wt%) and base oil (a). The COFs as a function of sliding velocity (b). Cross section of rubbing surfaces (c) and anti-wear properties under different lubrication conditions (d).

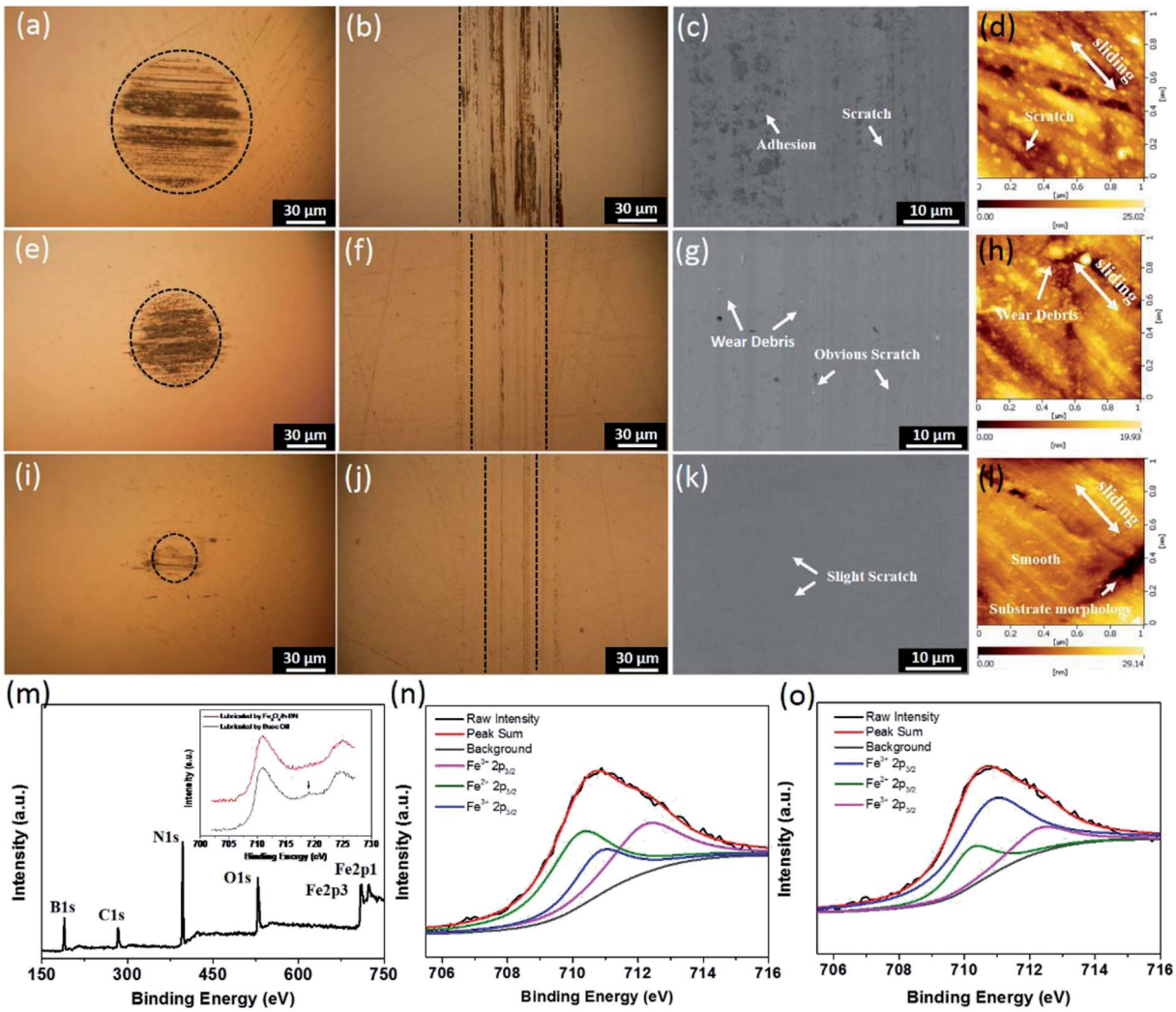

Fig. 5 Rubbing surfaces lubricated by base oil: optical micrographs (a and b), SEM image (c) and AFM image (d); rubbing surfaces lubricated by pure h-BN: optical micrographs (e and f), SEM image (g) and AFM image (h); rubbing surfaces lubricated by Fe_3O_4/h-BN: optical micrographs (i and j), SEM image (k) and AFM image (l); XPS spectra of rubbing surface lubricated by Fe_3O_4/h-BN (m) and the inset shows Fe 2p spectra, the analysis on the Fe 2p3/2 spectra from rubbing surfaces of Fe_3O_4/h-BN (n) and base oil (o).

region,[22] thereby resulting in obvious scratches and many wear debris shown in Fig. 5(g) and (h). According to the Fig. 5(k) and (l), the surface lubricated by the Fe_3O_4/h-BN is very smooth, and only some slight wear tracks appears on the contact region, which confirms that the Fe_3O_4/h-BN displays significant anti-wear properties. Based on the XPS results (Fig. 5(m)–(o)), the characteristic peaks of B 1s, N 1s, Fe 2p, O 1s and C 1s were clearly observed on the rubbing surfaces of Fe_3O_4/h-BN, which means that the Fe_3O_4/h-BN has synergetic lubricating effect and can form a synergetic tribofilm on the rubbing surfaces for friction and wear reduction. Furthermore, the Fe 2p spectrum from the rubbing surface of the base oil are shown in the inset of Fig. 5(m). There is obvious satellite peak at 719 eV which is a characteristic peak of Fe_2O_3, meaning that friction under the base oil results in many Fe_2O_3 scratches and Fe_2O_3 debris.[25] In contrast, under the lubrication of the Fe_3O_4/h-BN, there isn't obvious satellite peak, and the peaks of the Fe 2p spectrum generally shift to higher binding energy mainly attributed to Fe_3O_4.[26] In addition, the binding energy peak at 710.2 eV is attributed to Fe^{2+}, which is probably originated from Fe_3O_4. The peaks at 710.8 eV and 712.6 eV are from Fe^{3+} (ref. 27 and 28) as shown in Fig. 5(n) and (o). The surface lubricated by Fe_3O_4/h-BN shows a higher peak intensity of Fe^{2+} than the peak intensity from the lubrication of base oil, which confirm the Fe_3O_4 could be released from the Fe_3O_4/h-BN and formed a synergetic tribofilm on the rubbing surface together with h-BN.

Conclusion

In summary, the Fe_3O_4/h-BN 2D nanocomposite as a lubricant additive was prepared by a simple and low-cost route, in which the exfoliated h-BN nanosheets displays unique 2D-layered structure without folds or wrinkles and the Fe_3O_4 nanoparticles (4 nm) are uniformly dispersed on the h-BN nanosheet surfaces. The COF of lubricants and the wear depth of the rubbing surfaces lubricated by Fe_3O_4/h-BN can be respectively

reduced by 47% and 80% because of its synergetic lubricating effect. Therefore, this study offers an efficient synthesis method of Fe_3O_4/h-BN additives, which is of significant meaning for lubrication application due to not only the simple, low-cost route, but also the excellent tribological properties.

Conflicts of interest

There are no conflicts to declare.

Acknowledgements

This work is supported by grants from National Key Basic Research Program of China (973 Program) (No. 2014CB046404), Initiative Scientific Research Program of Materials Institute CAEP (TP02201704) and National Natural Science Foundation of China (51527901).

Notes and references

1 Z. Pawlak, T. Kaldonski, R. Pai, E. Bayraktar and A. Oloyede, *Wear*, 2009, **267**, 1198–1202.
2 J. Zhao, Y. He, Y. Wang, W. Wang, L. Yan and J. Luo, *Tribol. Int.*, 2016, **97**, 14–20.
3 D. Berman, A. Erdemir and A. V. Sumant, *Carbon*, 2013, **54**, 454–459.
4 Z. Chen, H. Yan, Q. Lyu, S. Niu and C. Tang, *Composites, Part A*, 2017, **101**, 98–107.
5 J. Zhao, J. Mao, Y. Li, Y. He and J. Luo, *Appl. Surf. Sci.*, 2018, **434**, 21–27.
6 J. Li, J. Li and J. Luo, *Adv. Sci.*, 2018, 1800810.
7 R. C. Sinclair, J. L. Suter and P. V. Coveney, *Adv. Mater.*, 2018, **30**, 1705791.
8 Y. Zhang, H. Tang, X. Ji, C. Li, L. Chen, D. Zhang, X. Yang and H. Zhang, *RSC Adv.*, 2013, **3**, 26086–26093.
9 H.-J. Song, X.-H. Jia, N. Li, X.-F. Yang and H. Tang, *J. Mater. Chem.*, 2012, **22**, 895–902.
10 A. K. Sharma, J. K. Katiyar, S. Bhaumik and S. Roy, *Friction*, 2018, **2018**(2), 1–16.
11 X. Wu, G. Zhao, Q. Zhao, K. Gong, X. Wang, W. Liu and W. S. Liu, *RSC Adv.*, 2016, **6**, 4–10.
12 X. Wu, K. Gong, G. Zhao, W. Lou, X. Wang and W. Liu, *RSC Adv.*, 2018, **8**, 4595–4603.
13 W. Jian, L. Mu, J. Zhu, F. Xin, X. Lu, R. Larsson and Y. Shi, *Carbon*, 2018, **134**, 423–430.
14 Y. Xu, Y. Peng, Y. Tao, L. Yao, G. Jian, K. D. Dearn and X. Hu, *Nanotechnology in Oil and Gas Industries*, Springer, Cham, 2018, pp. 151–191.
15 M. Thibaut, T. H. Tran, S. Szaffarczyk and M. Boucart, *Nano Lett.*, 2014, **14**, 3623–3627.
16 M. Iannuzzi, F. Tran, R. Widmer, T. Dienel, K. Radican, Y. Ding, J. Hutter and O. Gröning, *Phys. Chem. Chem. Phys.*, 2014, **16**, 12374–12384.
17 S. Kumari, O. P. Sharma, R. Gusain, H. P. Mungse, A. Kukrety, N. Kumar, H. Sugimura and O. P. Khatri, *ACS Appl. Mater. Interfaces*, 2015, **7**, 3708–3716.
18 Z.-Q. Duan, Y.-T. Liu, X.-M. Xie and X.-Y. Ye, *Chin. Chem. Lett.*, 2013, **24**, 17–19.
19 Z. Q. Duan, Y. T. Liu, X. M. Xie, X. Y. Ye and X. D. Zhu, *Chem.–Asian J.*, 2016, **11**, 828–833.
20 Y. T. Liu, X. M. Xie and X. Y. Ye, *Chem. Commun.*, 2013, **49**, 388–390.
21 C. Zhang, Y. He, F. Li, H. Di, L. Zhang and Y. Zhan, *J. Alloys Compd.*, 2016, **685**, 743–751.
22 J. Zhao, Y. Li, Y. Wang, J. Mao, Y. He and J. Luo, *RSC Adv.*, 2017, **7**, 1766–1770.
23 Y. Li, J. Zhao, C. Tang, Y. He, Y. Wang, J. Chen, J. Mao, Q. Zhou, B. Wang and F. Wei, *Adv. Mater. Interfaces*, 2016, **3**, 1600700.
24 J. Zhao, Y. Li, J. Mao, Y. He and J. Luo, *Tribol. Int.*, 2017, **116**, 303–309.
25 A. Erdemir, G. Ramirez, O. L. Eryilmaz, B. Narayanan, Y. Liao, G. Kamath and S. K. Sankaranarayanan, *Nature*, 2016, **536**, 67–71.
26 G. Sun, B. Dong, M. Cao, B. Wei and C. Hu, *Chem. Mater.*, 2011, **23**, 1587–1593.
27 D. Wilson and M. A. Langell, *Appl. Surf. Sci.*, 2014, **303**, 6–13.
28 R. Dedryvère, M. Maccario, L. Croguennec, F. d. r. L. Cras and D. Gonbeau, *Chem. Mater.*, 2008, **20**, 7164–7170.